COBEM 2023 27TH INTERNATIONAL CONGRESS OF MECHANICAL ENGENEERING

ABCM Brazilian Society of Mechanical Sciences and Engineering
27th ABCM International Congress of Mechanical Engineering
December 04-08, 2023, Florianópolis-SC, Brazil

COB-2023-0841
NUMERICAL INVESTIGATION OF DYNAMIC BEHAVIOR OF 1-D HIERARCHICAL METAMATERIALS

Cássio Bruno Florêncio Gomes
Federal Institute of Maranhão, IFMA-PPGEM, Avenida Getúlio Vargas, 4, CEP 65030-005, São Luís, MA, Brazil
cassio.bruno@acad.ifma.edu.br
Antônio Vinicius Garcia Campos
University of Campinas, UNICAMP-FEM-DMC, Rua Mendeleyev, 200, CEP 13083-970, Campinas, SP, Brazil.
Edilson Dantas Nóbrega
Federal University of Maranhão, UFMA-CCET-CCEM, Avenida dos Portugueses, 1966, CEP 65080-005, São Luís, MA, Brazil
edilson.dantas@ufma.br
Flávio Nunes Pereira
State University of Maranhão, UEMA-CCT-DEMEC, Rua Paulo VI, s/n, CEP 65055-970, São Luís, MA, Brazil
flaviomecn@yahoo.com.br
José Maria Campos dos Santos
University of Campinas, UNICAMP-FEM-DMC, Rua Mendeleyev, 200, CEP 13083-970, Campinas, SP, Brazil.
Edson Jansen Pedrosa de Miranda Jr.
Federal Institute of Maranhão, IFMA-EIB-DE, Rua Afonso Pena, 174, CEP 65010-030, São Luís, MA, Brazil
Federal Institute of Maranhão, IFMA-PPGEM, Avenida Getúlio Vargas, 4, CEP 65030-005, São Luís, MA, Brazil
Vale Institute of Technology, Rua Professor Paulo Magalhães Gomes - Bauxita, CEP 35400-000, Ouro Preto, MG, Brazil
edson.jansen@ifma.edu.br

Abstract. *Metamaterials are artificial structures designed to achieve performance over static or dynamic conditions that usual materials would not be able to accomplish. In mechanical structures, they are applied for noise control, vibration isolation, and wave attenuation, for example. Recently, the effect of hierarchy has been combined to the convenient properties offered by mechanical metamaterials. Therefore, in this work, the complex dispersion diagram and the forced response of flexural waves propagating in a 1-D hierarchical metamaterial Euler-Bernoulli beam are investigated. The influence of graded arrays of spring-mass resonators attached to the surface of a homogeneous beam on the formation of Bragg-type and locally resonant band gaps is studied. The plane wave expansion (PWE), extended plane wave expansion (EPWE), and wave finite element (WFE) approaches are used to compute the complex dispersion diagram of the hierarchical metamaterial beam with attached resonators. The forced response is computed by the spectral element (SEM), and WFEM approaches. The numerical results of all methods present good agreement. The hierarchy can improve both unit cell wave attenuation and vibration reduction of the metamaterial beam.*

Keywords: *Mechanical metamaterials, wave propagation, hierarchical structures, dispersion diagram, band gaps.*

1. INTRODUCTION

Mechanical metamaterials, also known as elastic metamaterials or locally resonant phononic crystals, are artificial materials designed to achieve unusual apparent mechanical performance, such as unusual static behaviour (*e.g.*, negative thermal expansion, negative Poisson's ratio) and extraordinary dynamic behaviour, for instance, acoustic wave transmission with expected band gaps or propagation paths, a unique combination of stiffness, strength and energy absorption performance, full-band mechanical vibration isolation, and others (Wu *et al.*, 2021).

An important property of mechanical metamaterials are the stop bands or band gaps in the dispersion diagram, which are frequency ranges where there are only evanescent modes. The band gaps in mechanical metamaterials are opened due to the local resonance phenomena and due to the Bragg scattering mechanism (whether the system is periodic). Locally resonant band gaps arise on the vicinity of resonator natural frequency and they do not depend on periodicity, while Bragg-type band gaps typically occur at wave lengths of the order of unit cell size.

There are many applications of mechanical metamaterials for solving engineering problems, such as vibration isolation and wave attenuation, acoustic purposes, heat transfer, and acoustic cloaking. With the advances of additive manufacturing and 3-D printing, the study and design of mechanical metamaterials have been a current research topic and bring promising prospects for engineering problems.

Hierarchical materials are those in which their structural elements themselves have a specific arrangement. They can be man-made or occur naturally. Therefore, understanding the effects of these hierarchies, it is possible to design materials

with physical properties tailored for specific applications (Lakes, 1993). Recently, the concepts of hierarchical materials and mechanical metamaterials have been combined and researchers found that hierarchy features in structures can modify the dynamic performance of metamaterials.

Gatt *et al.* (2015), proposed a type of hierarchical auxetic metamaterial based on the rotating rigid units mechanism capable of exhibit negative Poison's ratio that are candidates for industrial and biomedical applications, such as stents and skin grafts. Banerjee (2021), studied the effect of graded variation of mass and distance between successive resonators in a metabeam. He found that the flexural band-structure is highly sensitive to the natural frequency and the distance between the resonators, and that the low frequency band gaps are shifted or widened in this type of arrangement. Hu *et al.* (2021), investigated a graded metamaterial beam for broadband vibration suppression and conducted a parametric study to reveal the effects of the frequency spacing and damping ratio on the dynamic behaviour of the structure. The authors also proposed a design strategy using piezoelectric metamaterial beam to tune the frequency spacing to get a wide attenuation region. Thus, recently the concepts of hierarchical materials and mechanical metamaterials have been combined (Meza *et al.*, 2015), for realizing broadband vibration suppression (Xu *et al.*, 2019; Jafari *et al.*, 2020; Alshaqaq and Erturk, 2021). Other studies related to metamaterials with resonators have been held to investigate the dynamic performance in the context of vibration isolation and wave attenuation in order to obtain low frequency band gaps for 1-D (Nobrega *et al.*, 2016; Miranda Jr. and Dos Santos, 2019; Santo *et al.*, 2020) and 2-D (Miranda Jr. *et al.*, 2019, 2020; Jin *et al.*, 2022) structures.

In this work, the complex dispersion diagrams and the forced response are computed considering the flexural wave propagation in a 1-D hierarchical metamaterial Euler-Bernoulli beam. These results are presented in order to analyse the influence of hierarchical parameters in the opening of band gaps in the dispersion diagram of a metamaterial beam with attached resonators.

First, the dispersion diagrams are calculated by using the PWE, EPWE, and WFEM approaches. Next, the forced response is obtained by the SEM and WFEM. For comparison purposes, it is simulated a the forced responses of a bare beam, (a conventional material, not a metamaterial). So, three different hierarchical arrangements in the position of the resonators are assessed in a multiple resonator beam, *i. e.,* an arithmetic, a geometric, and a Fibonacci progressions.

2. MODELING

Due to limitation in the number of pages, as the formulation of the approaches are extensive, the equations presented in this paper are those ones which are shared by all numeric methods.

Figure 1 sketches the 1-D graded metamaterial beam with multiple periodic attached resonators.

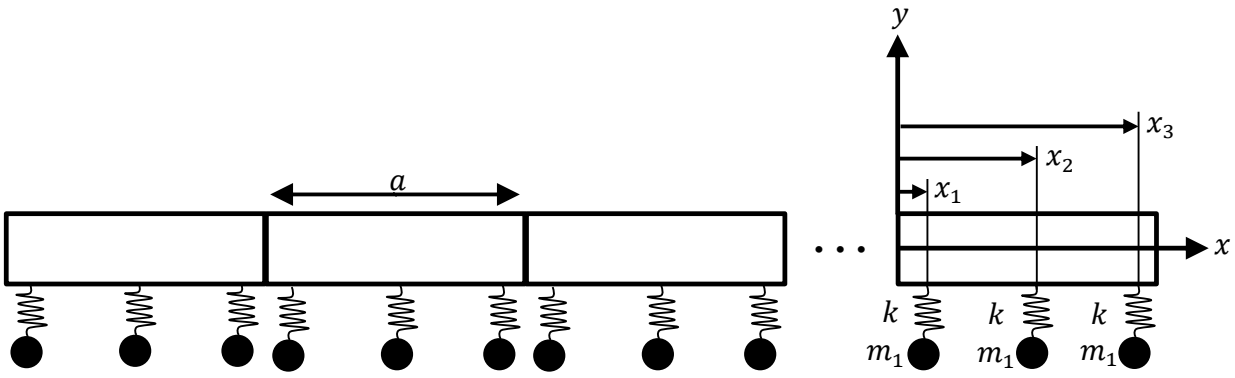

Figure 1. 1-D hierarchical metamaterial beam with multiple periodic resonators, where k is the stiffness, m_1 is the mass, x_j ($j = 1, 2, \ldots, N$) is the resonator's position, and a is the lattice constant.

In Fig. 1, there are N resonators at each unit cell with a lattice constant a. The resonators have the same stiffness k and the same mass m_1. The spatial position of the jth ($j = 1, 2, \ldots, N$) resonator at the unit cell is represented by x_j. The hierarchy is associated with the resonator position.

The Euler-Bernoulli beam theory (Doyle, 1997) is used to model a 1-D hierarchical metamaterial beam considering all approaches. According to this theory, the governing equation for flexural vibration of a uniform beam system can be written as Eq. (1):

$$\frac{\partial^2}{\partial x^2}\left[EI\frac{\partial^2 \hat{u}(x,t)}{\partial x^2}\right] + \rho S\ddot{\hat{u}}(x,t) = \hat{f}(x,t), \tag{1}$$

where $\hat{u}(x,t)$ is the transversal displacement in time domain, E is the Young's modulus, I is the second moment of area,

ρ is the density, S is the cross-sectional area of the beam, and $\hat{f}(x,t)$ is an external force, in this case, related to the spring-mass resonators with a single degree of freedom (SDOF).

Applying the temporal Fourier transform on Eq. (1), coupling the effect of the spring-mass resonators, and omitting frequency dependence ($u(x) = u(x,\omega)$ and $f(x) = f(x,\omega)$), where $\omega = 2\pi f$ is the angular frequency, one may write the flexural vibration of the metamaterial beam as Eq. (2):

$$EI\frac{\partial^4 u(x)}{\partial x^4} - \omega^2 \rho S u(x) = \sum_{j=1}^{N}\sum_{n=-\infty}^{+\infty} f_j(x_j + na)\delta[x - (x_j + na)], \tag{2}$$

where $u(x)$ and $f(x)$ are the Fourier transforms of $\hat{u}(x,t)$ and $\hat{f}(x,t)$. Also, $f_j(x_j + na)$ is the resonator force applied to the beam placed in the position $x_j + na$ and δ corresponds to the Dirac delta function. For multiple periodic arrays of attached SDOF spring-mass local resonators, the $f_j(x_j + na)$ can be expressed as Eqs. (3), and (4):

$$f_j(x_j + na) = -k_j\left[u(x_j + na) - w_j(x_j + na)\right],\ j = 1,\ 2,\ \ldots,\ N \tag{3}$$

$$-\omega^2 m_j w_j(x_j + na) = f_j(x_j + na),\ j = 1,\ 2,\ \ldots,\ N \tag{4}$$

where $w(x_j + na)$ is the displacement of the mass of jth resonator.

Due to the system periodicity, one can apply the Floquet-Bloch's theorem, decribed by Eq. (5):

$$u(x) = e^{i\kappa x}u_\kappa(x), \tag{5}$$

where $u_k(x)$ is the Bloch wave amplitude and $i = \sqrt{-1}$ is the complex unity. As the system is periodic, $u_\kappa(x) = u_\kappa(x+a)$ and $u(x + a) = u(x)e^{i\kappa a}$, where the exponential $e^{i\kappa a}$ is called Floquet-Bloch's periodic boundary condition, the wave number κ, also known as the Bloch wave vector, is restricted to the first Brillouin zone (FBZ), $[-\pi/a, \pi/a]$, or first irreducible Brillouin zone (FIBZ), $[0, \pi/a]$.

The PWE (Cao *et al.*, 2004), $\omega(k)$, and EPWE (Hsue *et al.*, 2005), $k(\omega)$, are used to compute the propagating and complex modes of the dispersion diagram, respectively. PWE is considered as a semi-analytical approach and returns only the propagating modes ($\Im\{k\} = 0$). Then, the EPWE approach overcomes this limitation, obtaining evanescent modes, that is, imaginary and complex values of k. To obtain the results in this article. three plane waves were used for the spatial Fourier series expansion for both PWE and EPWE.

The spectral element (SEM) method is based on the analytical solution of the displacement wave equation, written in the frequency domain (Doyle, 1997; Lee, 2009). The element is tailored in the same concept as finite element (FE) method, but the interpolation function is the exact (or approximated) solution of wave equation. Built-up structures with geometrically uniform members can be modelled by a single spectral element reducing significantly the total number of degrees of freedom (DOFs) as compared to the approximated approaches.

The WFEM (wave finite element method) is a wave propagation method applicable to periodic structures. It involves removing a slice of the structure and then calculating the frequencies and propagation modes of the wave in that slice using FE, from which the amplitudes of the wave are determined and the displacements are found. Nascimento (2009), combined the SE with the FE method, resulting in a semi-analytical method called WSE. But this method was still restricted to simple structures, since for modelling complex structures it was required cumbersome analytical formulations. However, this problem was circumvented by (Silva, 2015), who built spectral finite elements from a finite element model of a slice of a structural wave guide with an arbitrary cross section and, potentially, of arbitrary order.

3. NUMERICAL RESULTS

This section presents the numerical results for the complex dispersion diagram and the forced response using the approaches mentioned. This study consider ten resonators in a unit cell ($N = 10$), the mass (m_1) and spring stiffness (k) are $0.54{\cdot}10^{-3}$ kg and $4.51{\cdot}10^{3}$ N/m, respectively. The resonator natural frequency ($f_r = \sqrt{(k/m_1)}/2\pi$) is set in 460 Hz. The hierarchy is associated with the resonator position, considering arithmetic, geometric progressions, and a Fibonacci sequence, respectively. The metamaterial beam geometry and material properties are shown in Table 1.

3.1 Arithmetic progression

The arithmetic progression associated with the position of the resonators in the metamaterial Euler-Bernoulli beam can be expressed by Eq. (6):

$$x_j = x_1 + d(j-1), \tag{6}$$

where, $x_1 = 0$ is the position of the first resonator, placed at the first end of the model, x_j ($j = 1, 2, \ldots, 10$) is the position of the jth resonator, and $d = a/N$ is the ratio between the unit cell length of the beam and the number of resonators.

Table 1. Metamaterial beam geometry and material properties (Miranda Jr. and Dos Santos, 2019).

Geometry/Property	Value
Unit-cell length (a)	0.1 m
Cross-sectional area (A)	4×10^{-5} m^2
Young's modulus (E)	7×10^{10} Pa
Structural damping (η)	0.01
Mass density (ρ)	2700 kg/m^3
Second moment of area (I)	1.33×10^{-11} m^4

The dispersion diagram of the metamaterial beam with attached resonators, following an arithmetic progression in their position is shown in Figures 2 and 3. Figure 2(a) illustrates the dispersion diagram of the real part of normalized ($\kappa a/2\pi$) wave number versus frequency calculated by PWE ($\omega(k)$) using M = 3 harmonic terms in the Fourier series expansion, which means 3 plane waves. At low frequency bands a small number of harmonic terms is enough to achieve good convergence using the PWE and EPWE (Miranda Jr. and Dos Santos, 2019; Xiao *et al.*, 2012).

Figure 2(b) shows the imaginary part of the wave number, or the evanescent modes, calculated by EPWE ($k(\omega)$). The results show the presence of one band gap in the metamaterial beam, around 480 Hz. Due to the periodicity, a Bragg's type band gap is also expected and can be obtained by:

$$f_B = \frac{1}{2\pi}\left(\frac{\pi}{a}\right)^2 \sqrt{\frac{EI}{\rho A}} \approx 461.8 \text{ Hz}. \tag{7}$$

As the resonator frequency is near to the first Bragg's band gap frequency, it is obtained a coupling of the local resonance and Bragg's type band gaps. As a result of this combination, it is opened a wider band gap region and it is obtained higher attenuation of propagating waves.

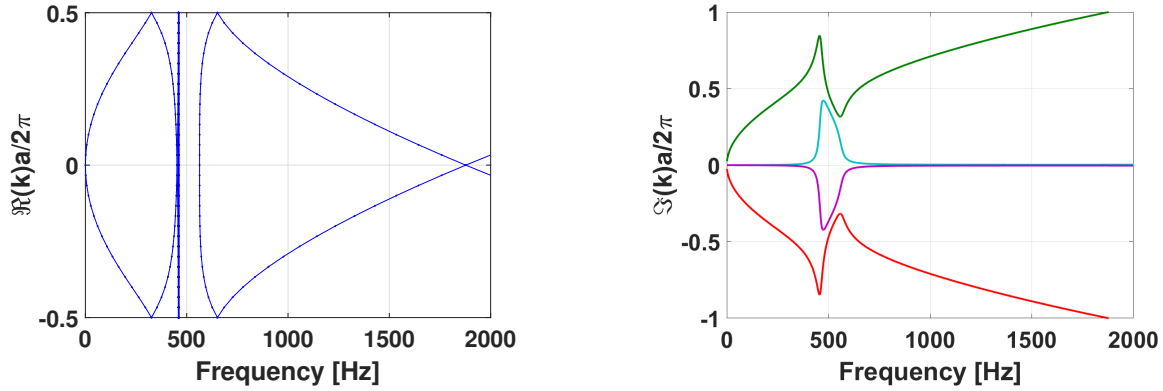

(*a*) (*b*)

Figure 2. Real (a) and imaginary (b) parts of the dispersion diagram for an arithmetic progression in resonator position calculated by PWE and EPWE, respectively.

Figure 3 shows the dispersion diagram for the metamaterial beam calculated by WFE. The normalized results for both real – propagating modes – characterized by the positive part the complex wave number, and imaginary, characterized by the negative part of the complex wave number, were obtained. Through this method, it was obtained a band gap in the same region than the one calculated by PWE and EPWE (Fig. 2) showing the coupling between Bragg's type and local resonance band gaps, as well as it is observed that the methods present good agreement.

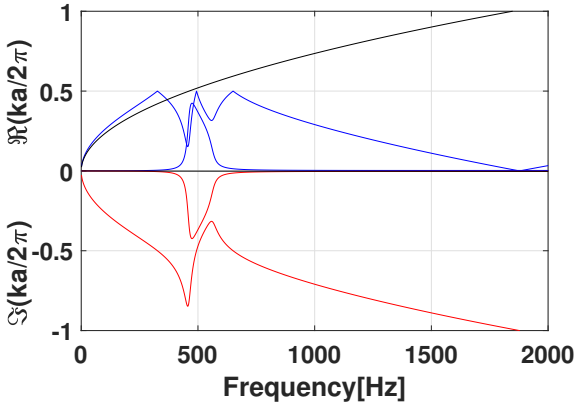

Figure 3. Complex dispersion diagram for an arithmetic progression of resonator's position calculated by WFEM.

3.2 Geometric progression

For the geometric progression, the resonator position along the metamaterial beam can be expressed as:

$$x_j = x_1 r^{j-1}, \tag{8}$$

where $x_1 = a/550$ is the position of the first resonator and $r = 2$ is the common ratio.

Figure 4 shows the dispersion diagram, that is, the reduced wave number versus frequency for a metamaterial beam with geometric progression hierarchy in resonator's position. The real part of wave number is obtained by PWE and it is shown in Fig. 4(a). On the other hand, EPWE approach was used to obtain the non real part of wave number, where one can assess the attenuation bands, and it is shown in Fig. 4(b). For this resonator's position arrangement, it is obtained two regions of band gaps. The first one near to 460 Hz, where occur the coupling of local resonance and Bragg's type band gaps. A second and tiny Bragg's band gap is observed in the range of 1850 Hz and 1900 Hz.

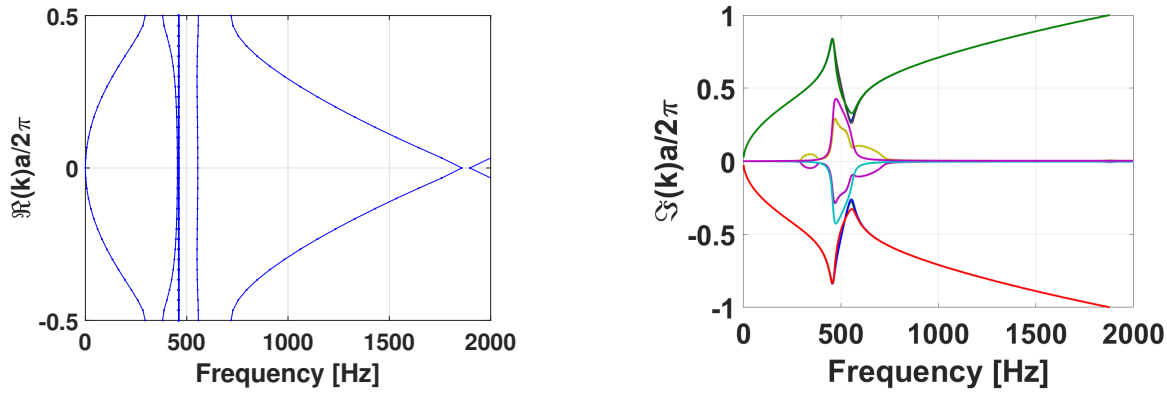

(*a*) (*b*)

Figure 4. Real (a) and imaginary (b) parts of the dispersion diagram for a geometric progression in resonator's position calculated by PWE and EPWE, respectively.

Figure 5 shows the dispersion diagram for the geometric progression in resonator's position calculated by WFEM. The non-zero imaginary part of Bloch's vector characterizes the frequency regions where the wave propagation is mostly governed by evanescent modes. Comparing to the arithmetic progression of resonator's position, while it is observed a wider band gap, the amplitude of the non-zero imaginary part is smaller. Because of that, for this arrangement, there is less wave attenuation than for an arithmetic progression. Finally, the results for all methods presented good agreement.

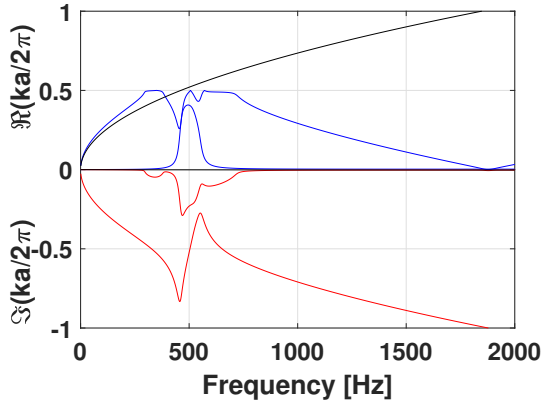

Figure 5. Complex dispersion diagram for a geometric progression of resonator's position calculated by WFEM.

3.3 Fibonacci sequence

For the last type of hierarchy, the Fibonacci sequence in the resonator position is given by:

$$x_1 = 0, x_k = \frac{\phi^k - \psi^k}{\sqrt{5}}, \tag{9}$$

$$x_j = \{x_1 \;\; x_k\}(a/4N), \tag{10}$$

where $k = 1, 2, \ldots, 9$, x_j is the position of the jth resonator respecting the Fibonacci sequence along the beam, $\phi = (1 + \sqrt{5})/2$ and $\psi = (1 - \sqrt{5})/2$ are the known as the golden ratio and its conjugate, respectively.

Figure 6 shows the dispersion diagram of the real (a) and imaginary (b) part of reduced wave number versus frequency for a Fibonacci sequence in the resonator's position. Again, there are two band gap regions, one near to the resonator's natural frequency, which couples both local resonance and Bragg's type effects. The other one is a narrow Bragg's band gap, opened around 1860 Hz due to the periodicity of the system.

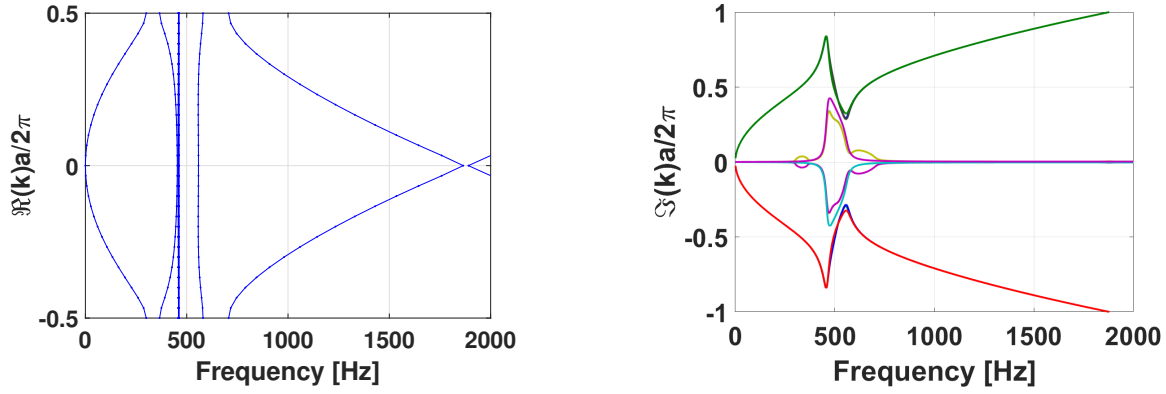

(*a*) (*b*)

Figure 6. Real (a) and imaginary (b) parts of the dispersion diagram for a Fibonacci sequence in resonator's position calculated by PWE and EPWE, respectively.

Figure 7 shows the dispersion diagram calculated by WFEM for a metamaterial beam with attached resonators following a Fibonacci sequence on the position. This result agrees with the PWE and EPWE approaches, and is also observed the coupling of Bragg's and local resonance band gaps.

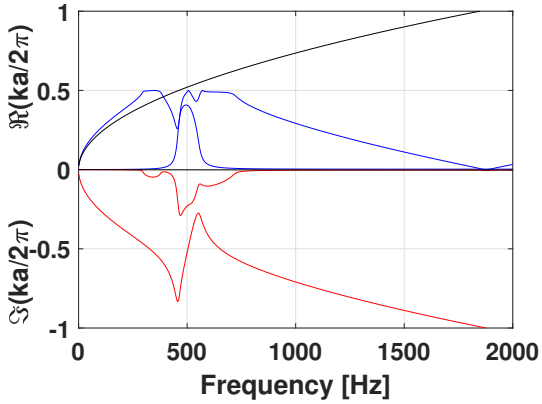

Figure 7. Complex dispersion diagram for a Fibonacci sequence of resonator's position calculated by WFEM.

3.4 Forced response

The forced response is useful to understand the dynamic behavior and vibration attenuation in finite structures. Through this dynamic response, one can assess the behavior of the system over non-static conditions. Additionally, attenuation zones can also be observed in this results.

Figure 8 exhibit the receptance in dB of a free-free metamaterial beam, excited in the first end and measured right at the point of the excitation. In Figs. 8(a), (b), and (c), the dashed blue lines corresponds to the forced response of a bare beam, *i.e.,* a conventional Euler-Bernoulli beam with no resonators attached, calculated by SEM, in order to observe the effect of attaching resonators in a beam. The solid red lines corresponds to the metamaterial beam with resonators placed in arithmetic, geometric, and Fibonacci sequences, respectively, and were obtained by WFEM.

The results show the same band gaps regions observed in the dispersion diagrams calculated by PWE, EPWE, and WFEM methods, thus validating the approach used to describe the dynamic behavior of the proposed structure. Figure 8(d) presents a zoom in frequency axis of the frequency response functions (FRFs) of the hierarchies studied, in order to notice the influence of the disposition of resonator's position in dynamic behaviour of the hierarchical metamaterial beams. Thus, the results exhibit that geometric progression in the resonator's position provides a wider band gap region than the other hierarchies studied.

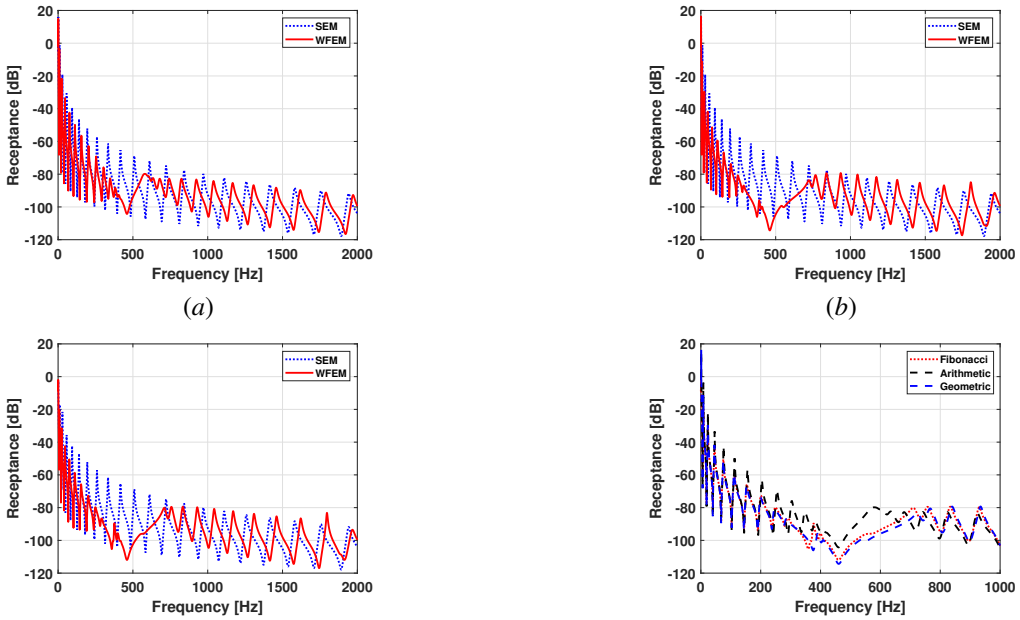

Figure 8. Forced response functions (FRFs) calculated by SEM (dashed blue lines - bare beam) and WFEM (solid red lines - hierarchical metamaterial) for arithmetic progression (a), geometric progression (b) and Fibonacci sequence (c). The FRFs comparison (d) between all hierarchies studied.

4. CONCLUSIONS

This work evaluated different types of hierarchy in the position of SDOF resonators along a metamaterial Euler-Bernoulli beam in order to create locally resonance and Bragg-type band gaps. For that, it were obtained dispersion diagrams for real and complex parts of wave number and the forced responses of a hierarchical metamaterial beam with attached resonators in a unit cell, using PWE, EPWE, WFEM, and SEM approaches, which presented good agreement in both dispersion diagrams and forced responses.

The simulated models and numerical calculations demonstrated a coupling between Bragg-type and locally resonance band gaps, due to the tuned natural frequency of the resonator. Although, the results shows that the band gap location or range is sensible to the disposition of the resonator along the unit cell.

Among the types of hierarchies studied – arithmetic, geometric and Fibonacci sequence – in the resonator position, the arithmetic progression presented a higher unit cell wave attenuation value *i. e.* with respect to the imaginary part of κ, even if occurs in a smaller frequency range. Geometric an Fibonacci sequences presented similar results, with wider band gaps and less amplitude of the imaginary part of wave number than the arithmetic progression.

5. ACKNOWLEDGEMENTS

The authors thank the Federal Institute of Maranhão (IFMA), Brazilian funding agencies CAPES (Finance Code 001), CNPq (Grant Reference Numbers 313620/2018, 151311/2020-0, 403234/2021-2, 405638/2022-1, and 300166/2022-2), FAPEMA (Grant Reference Numbers 07168/22 and 09683/22), and FAPESP (Grant Reference Number 2018/15894-0).

6. REFERENCES

Alshaqaq, M. and Erturk, A., 2021. "Graded multifunctional piezoelectric metastructures for wideband vibration attenuation and energy harvesting". *Smart Materials and Structures*, Vol. 30, p. 015029. doi:http://dx.doi.org/10.1088/1361-665X/abc7fa.

Banerjee, A., 2021. "Flexural waves in graded metabeam lattice". *Physics Letters A*, Vol. 388, p. 127057. doi:http://dx.doi.org/10.1016/j.physleta.2020.127057.

Cao, Y., Hou, Z. and Liu, Y., 2004. "Convergence problem of plane-wave expansion method for phononic crystals". *Physics Letters A*, Vol. 327, pp. 247–253. doi:http://dx.doi.org/10.1016/j.physleta.2004.05.030.

Doyle, J.F., 1997. *Wave Propagation in Structures: Spectral Analysis Using Fast Discrete Fourier Transforms*. Springer, Berlin, Germany.

Gatt, R., Mizzi, L., Azzopardi, J.I., Azzopardi, K.M., Attard, D., Casha, A., Briffa, J. and Grima, J.N., 2015. "Hierarchical auxetic mechanical metamaterials". *Scientific Reports*, Vol. 5, No. 8395. doi:http://dx.doi.org/10.1038/srep08395.

Hsue, Y.C., Freeman, A. and Gu, B.Y., 2005. "Extended plane-wave expansion method in three-dimensional anisotropic photonic crystals". *Physical Review B*, Vol. 72, p. 195118. doi:http://dx.doi.org/10.1103/PhysRevB.72.195118.

Hu, G., Austin, A.C.M., Sorokin, V. and Tang, L., 2021. "Metamaterial beam with graded local resonators for broadband vibration suppression". *Mechanical Systems and Signal Processing*, Vol. 146, p. 106982. doi:http://dx.doi.org/10.1016/j.ymssp.2020.106982.

Jafari, H., Sepehri, S., Yazdi, M.R.H., Mashhadi, M.M. and Fakhrabadi, M.M.S., 2020. "Hybrid lattice metamaterials with auxiliary resonators made of functionally graded materials". *Acta Mechanica*, Vol. 231, pp. 4835–4849. doi:http://dx.doi.org/10.1007/s00707-020-02799-0.

Jin, Y., Jia, X.Y., Wu, Q.Q., Yu, G.C., Zhang, X.L., Chen, S. and Wu, L.Z., 2022. "Design of cylindrical honeycomb sandwich meta-structures for vibration suppression". *Mechanical Systems and Signal Processing*, Vol. 163, p. 108075. doi:http://dx.doi.org/10.1016/j.ymssp.2021.108075.

Lakes, R., 1993. "Materials with structure hierarchy". *Nature*, Vol. 361, pp. 511–515. doi:https://doi.org/10.1038/361511a05.

Lee, U., 2009. *Spectral Element Method in Structural Dynamics*. John Wiley and Sons (Asia), Singapore.

Meza, L.R., Zelhofer, A.J., Clarke, N., Mateos, A.J., Kochmann, D.M. and Greer, J.R., 2015. "Resilient 3D hierarchical architected metamaterials". *PNAS*, Vol. 112, No. 37, pp. 11502–11507. doi:http://dx.doi.org/10.1073/pnas.1509120112.

Miranda Jr., E.J.P. and Dos Santos, J.M.S., 2019. "Flexural wave band gaps in multi-resonator elastic metamaterial Timoshenko beams". *Wave Motion*, Vol. 91, p. 102391. doi:http://dx.doi.org/10.1016/j.wavemoti.2019.102391.

Miranda Jr., E.J.P., Nobrega, E.D., Ferreira, A.H.R. and Dos Santos, J.M.S., 2019. "Flexural wave band gaps in a multi-resonator elastic metamaterial plate using Kirchhoff-Love theory". *Mechanical Systems and Signal Processing*, Vol. 116, pp. 480–504. doi:http://dx.doi.org/10.1016/j.ymssp.2018.06.059.

Miranda Jr., E.J.P., Nobrega, E.D., Rodrigues, S.F., Aranas Jr., C. and Dos Santos, J.M.S., 2020. "Wave attenuation in elastic metamaterial thick plates: Analytical, numerical and experimental investigations". *International Journal of Solids and Structures*, Vol. 204–205, pp. 138–152. doi:http://dx.doi.org/10.1016/j.ijsolstr.2020.08.002.

Nascimento, R., 2009. *Propagação de ondas utilizando modelos de elementos finitos em guias de onda estruturais (in*

Portuguese). Ph.D. thesis, Graduate Program in Mechanical Engineering, University of Campinas, Campinas, Brasil.

Nobrega, E.D., Gautier, F., Pelat, A. and Dos Santos, J.M.C., 2016. "Vibration band gaps for elastic metamaterial rods using wave finite element method". *Mechanical Systems and Signal Processing*, Vol. 79, pp. 192–202. doi: http://dx.doi.org/10.1016/j.ymssp.2016.02.059.

Santo, D.R., Mencik, J.M. and Gonçalves, P.J.P., 2020. "On the multi-mode behavior of vibrating rods attached to nonlinear springs". *Nonlinear Dynamics*, Vol. 100, pp. 2187–2203. doi:http://dx.doi.org/10.1007/s11071-020-05647-x.

Silva, P., 2015. *Dynamic analysis of periodic structures via wave-based numerical approaches and substructuring techniques*. Ph.D. thesis, Graduate Program in Mechanical Engineering, University of Campinas, Campinas, Brasil.

Wu, L., Wang, Y., Chuang, K., Wu, F., Wang, Q., Lin, W. and Jiang, H., 2021. "A brief review of dynamic mechanical metamaterials for mechanical energy manipulation". *Materials Today*, Vol. 44, pp. 168–193. doi: http://dx.doi.org/10.1016/j.mattod.2020.10.006.

Xiao, Y., Wen, J. and Wen, X., 2012. "Broadband locally resonant beams containing multiple periodic arrays of attached resonators". *Physics Letters A*, Vol. 376, No. 16, pp. 1384–1390. ISSN 0375-9601. doi:https://doi.org/10.1016/j.physleta.2012.02.059. URL `https://www.sciencedirect.com/science/article/pii/S037596011200254X`.

Xu, X., Barnhart, M.V., Li, X., Chen, Y. and Huang, G., 2019. "Tailoring vibration suppression bands with hierarchical metamaterials containing local resonators". *Journal of Sound and Vibration*, Vol. 442, pp. 237–248. doi: http://dx.doi.org/https://doi.org/10.1016/j.jsv.2018.10.065.

7. RESPONSIBILITY NOTICE

The authors are solely responsible for the printed material included in this paper.